



ELSEVIER

31 March 2000

**CHEMICAL  
PHYSICS  
LETTERS**

Chemical Physics Letters 320 (2000) 186–193

www.elsevier.nl/locate/cplett

# Liquid structure at metal oxide–water interface: accuracy of a three-dimensional RISM methodology

Vladimir Shapovalov <sup>a</sup>, Thanh N. Truong <sup>a,\*</sup>, Andriy Kovalenko <sup>b,1</sup>, Fumio Hirata <sup>b</sup><sup>a</sup> *Henry Eyring Center for Theoretical Chemistry, Department of Chemistry, University of Utah, 315 S 1400 E, Rm Dock, Salt Lake City, UT 84112, USA*<sup>b</sup> *Institute for Molecular Science, Myodaiji, Okazaki 444-8585, Japan*

Received 28 September 1999; in final form 22 January 2000

## Abstract

We calculated the structure of water in contact with the MgO(100) surface by using the three-dimensional reference interaction site model (3D-RISM) integral equation theory. The spatial distributions of water oxygen and hydrogen over the surface unit cell are calculated and discussed. The water density profiles and the orientations obtained are in good agreement with computer simulations for the same model of the interface. The 3D-RISM approach shows considerable promise as a constituent of a self-consistent description of chemical processes at a metal oxide–water interface. © 2000 Elsevier Science B.V. All rights reserved.

## 1. Introduction

The chemistry at metal oxide–water interfaces is critically important in many industrial and environmental processes such as interactions at mineral oxides–water interfaces governing the hydrodynamics of species in the Earth's subsurface. It is known that the role of liquid water is crucial in understanding the structure and activity of such interfaces. Consequently, the ability to predict liquid structure at the metal oxide–water interface is of great importance.

In this study, we present an investigation on the accuracy of a three-dimensional reference interaction site model (3D-RISM) approach in predicting the liquid structure at the MgO(100)–water interface.

This work is motivated by the need for an accurate theoretical model that can treat chemical reactions at solid–liquid interfaces. Several methodologies [1–3] proposed recently have shown to be promising but do have certain drawbacks. The RISM method which is an orientational reduction of the molecular Ornstein–Zernike (OZ) integral equation [4] can provide a realistic description for molecular liquids of various complexity. This method was pioneered by Chandler and Andersen [5], and then extended by Hirata and co-workers to polar and quadrupolar liquids [6,7] and to ions in a molecular polar solvent [8] by adapting the hypernetted chain (HNC) closure. A great advantage of the RISM method over other integral equation theories for molecular liquids [4] is that it can easily handle the description of solution comprising complex polyatomic species, such as polar or nonpolar organic molecules and molecular ions, and to take into account such chemical specificities as hydrogen bonding [9]. In the case of a

\* Corresponding author. Fax: +1-801-581-4353; e-mail: truong@mercury.hec.utah.edu

<sup>1</sup> Present address: Henry Eyring Center for Theoretical Chemistry, Department of Chemistry, University of Utah.

solid–molecular liquid interface, however, spatial distributions of liquid are required rather than radial correlation functions produced by the site–site RISM approach. A detailed solvation structure in the form of three-dimensional (3D) correlation functions of interaction sites of solvent molecules near a solute particle of arbitrary shape is yielded by the 3D generalization of the RISM integral equation theory, first derived by Chandler et al. in a general form within the density functional method for nonuniform polyatomic systems [10,11], and recently developed by Cortis et al. for a one-component dipolar liquid [12], Beglov and Roux for water and organic molecules in water [13], and Kovalenko and Hirata for water [14,15], molecular ions in a polar organic solvent [16], and metal–water interfaces [14,17].

In this study, we propose to incorporate the 3D-RISM integral equation theory to model the liquid phase at metal oxide–liquid interfaces. Hirata and co-workers successfully combined the RISM formalism with ab initio molecular orbital methods to study physical and chemical processes including reactions in solution [9,18–22]. Kovalenko and Hirata have coupled the 3D-RISM and Kohn–Sham DFT methods to self-consistently describe the electronic and classical structure of a metal–liquid interface [17]. However, before we attempt to employ this combined approach to study solid–liquid interfaces, it would be of great interest to test the accuracy of the 3D-RISM formalism in modeling the liquid phase in contact with a metal oxide surface. We consider the MgO(100)–water interface because of the extensive work done for this system both theoretically and experimentally. In particular, McCarthy and co-workers have developed an accurate ab initio-derived molecular mechanics force field for interactions of a water molecule with the MgO(100) surface, and have performed combined MD–MC simulations to obtain the structure of water at the MgO surface [23]. The latter will be used as a reference point for the comparison.

## 2. Three-dimensional RISM equations for the structure of a molecular liquid in contact with a solid

In this work we employ the 3D-RISM/PLHNC integral equation theory developed recently by Ko-

valenko and Hirata [16,17], and only briefly described here. The MgO slab is regarded as a single ‘solute’ immersed in water ‘solvent’. At infinite dilution, the 3D-RISM integral equation for the 3D ‘solute–solvent’ correlations is written as

$$h_\gamma(\vec{r}) = c_\alpha(\vec{r}) * [\omega_{\alpha\gamma}(r) + \rho h_{\alpha\gamma}(r)], \quad (1)$$

where  $h_\gamma(\vec{r})$  and  $c_\gamma(\vec{r})$  are the 3D total correlation and direct correlation functions of solvent site  $\gamma$  around the solute,  $\omega_{\alpha\gamma}(r)$  is the solvent intramolecular correlation matrix,  $\rho$  is the solvent density, and ‘\*’ denotes convolution in coordinate space and summation over repeating site indices. The radial total correlation function between sites  $\alpha$  and  $\gamma$  of two molecules of pure solvent,  $h_{\alpha\gamma}(r)$ , is obtained from the conventional, site–site RISM/HNC integral equations [6–9,24]. Similarly to the site–site RISM theory, a 3D-HNC closure to the 3D-RISM Eq. (1) can be constructed [10–17]. The 3D-RISM/HNC approximation proved to yield physically reasonable results for charged as well as neutral solutes in polar solvents, in particular in water, at normal conditions [12–16]. However, it can become divergent in the case of molecular ions and planar interfaces with high local charges creating deep potential wells for individual interaction sites of polar solvent molecules [16,17]. This is of particular importance in the present case of the MgO surface comprising doubly charged ions  $\text{Mg}^{2+}$  and  $\text{O}^{2-}$ . To eliminate this shortcoming, Kovalenko and Hirata proposed the partial linearization of the HNC closure (PLHNC approximation) [16,17],

$$g_\gamma(\vec{r}) = \begin{cases} \exp(p_\gamma(\vec{r})) & \text{for } p_\gamma(\vec{r}) \leq 0, \\ 1 + p_\gamma(\vec{r}) & \text{for } p_\gamma(\vec{r}) > 0, \end{cases} \quad (2a)$$

$$p_\gamma(\vec{r}) = -\beta u_\gamma(\vec{r}) + h_\gamma(\vec{r}) - c_\gamma(\vec{r}), \quad (2b)$$

where  $g_\gamma(\vec{r}) = h_\gamma(\vec{r}) + 1$  is the 3D distribution function of solvent site  $\gamma$  around the solute,  $u_\gamma(\vec{r})$  is the 3D solute–solvent potential at solvent site  $\gamma$  in the field of the entire solute, which is a sum of the pairwise potentials between solvent site  $\gamma$  and solute ions constituting the MgO slab, and  $\beta = 1/kT$ . The distribution function  $g_\gamma$  and its first derivative are continuous at the joint point  $p_\gamma = 0$  by construction. In fact, it combines the exponential, HNC closure for

the regions of density profile depletion,  $h_\gamma(\vec{r}) < 0$ , and a type of the linear, Percus–Yevick (PY) approximation for the regions of enrichment,  $h_\gamma(\vec{r}) > 0$ . Notice that unlike the true PY closure, the PLHNC approximation linearizes the *entire* exponent,  $\exp(-\beta u + h - c)$  for  $h > 0$ , including the potential term,  $-\beta u$ . The PLHNC approximation (6) provides proper account of the long-range asymptotics of the direct correlation functions similarly to the original HNC closure, but prevents the exponential rise of the distribution function in the regions of a large potential bringing about the divergence. Besides ensuring convergence, under normal conditions this partial linearization results in some reduction and slight widening of high peaks at the distribution functions. The latter inhibits a noticeable change of the coordination numbers of the solvation shells [17].

### 3. Model and computational details

The system is modeled by a unit cell of size  $2.97 \times 2.97 \times 30.0 \text{ \AA}$  containing a slab of five MgO layers. With the periodic boundary conditions applied in three dimensions, it produces infinite slabs of MgO separated by layers of water  $\sim 21.5 \text{ \AA}$  thick. We used the lattice constant  $a = 4.205 \text{ \AA}$  and the atomic pair potentials published by McCarthy et al. [23] to allow for direct comparison with their simulation results. The pairwise interactions between the MgO slab ions and the water interaction sites are represented by the Huggins–Mayer potential with the parameters taken from Ref. [23]. The electrostatic part of the periodic potential (5) between the whole MgO slab and the water sites is synthesized on the supercell grid by using the Ewald summation method [25]. The other terms of the Huggins–Mayer potential as well as the short-range part of the Ewald sum are summed in direct space over the central and nearest adjacent unit cells. The interaction between water sites is described with the sum of the Coulomb and Lennard-Jones (LJ) potentials, and the LJ parameters for unlike water sites are determined by the standard mixing rules. We employed the simple point charge (SPC) water model [26]. The only modification is that a LJ size of  $\sigma_H = 1 \text{ \AA}$  is introduced for the hydrogen sites. This does not affect the entire potential between a pair of water molecules since the

hydrogens are situated well inside the oxygen core, however allows one to improve the description of hydrogen bonds by the RISM theory [22,27].

The 3D-RISM/PLHNC integral equations for the solute–solvent correlations are solved on a 3D grid of  $16 \times 16 \times 128$  points which gives the resolution of  $0.19 \text{ \AA}$  along the MgO surface, and  $0.23 \text{ \AA}$  in the direction perpendicular to it. The convolution in Eq. (1) is handled by using the 3D fast Fourier transform [28]. The site-site RISM/HNC integral equations for the correlations of pure water are solved on a radial non-linear grid of 512 points by using the standard technique of the nonlinear 1D fast Fourier transform [29,30]. In solving both the site–site RISM and 3D-RISM equations, we do not need the renormalization technique [14–17]. We also avoid the so-called ‘cooling’ and ‘charging’ procedures of gradually decreasing the temperature and increasing the molecular charges [6–8,12,13]. Due to the choice of the trial functions, the solution process starts at once from a given temperature and the full charges of the interaction sites, which greatly reduces the computation time [14–17].

To converge the 3D-RISM equations for the MgO–water correlations as well as the conventional RISM equations for bulk water, we employed the modified direct inversion in the iterative subspace (MDIIS) method elaborated in the context of liquid structure calculations by Kovalenko et al. [15,16] which is based on the DIIS method proposed originally by Pulay [31–33] for ab initio molecular orbital calculations. Maw et al. [22] used the DIIS procedure for the first time to solve the site–site RISM integral equations for water correlations. The main MDIIS improvement to the original DIIS consists in updating the DIIS subspace at every iterational step by using the approximated minimal residual scaled by a factor, rather than simply by performing damped iterations. Recently, Kawata et al. [34] have proposed to update the DIIS basis by the modified Broyden (MB) multidimensional secant method, and applied this combined DIIS-MB scheme to solve the 3D-RISM integral equations for nonpolar and polar diatomic  $N_2$ -like molecules. The MB update considerably improves the DIIS-MB convergence rate as compared to the original DIIS method with the iterational update. However, we do not expect that in general the MB update could offer an essential ad-

vantage over the MDIIS procedure. As was pointed out by Hamilton and Pulay [33], the DIIS technique is very close to conjugate-gradient type methods. Therefore, the successive DIIS minimization by itself improves and optimizes the MDIIS update. More discussion on this point as well as details of the MDIIS procedure can be found in Refs. [15,16]. The MDIIS method provides great acceleration of convergence as compared to Picard-type iterations, which is especially important and constitutes a challenging task in the case of 3D integral equations. We obtained the 3D site water–surface distributions within root mean square accuracy of  $4 \times 10^{-5}$  in  $\sim 70$  MDIIS iterations with the MDIIS subspace of 10 vectors. For  $2^{15}$  grid-points, the calculation needs 11 Mbytes of memory and takes  $< 5$  min on a RISC 6000 workstation. This is significantly less than that would be required for MD/MC simulation.

#### 4. Results and discussion

From the simulations for 128 water molecules, McCarthy et al. [23] pointed out two particular features of water density distribution functions above the MgO surface that are distinctively different from those of the bulk water. One is a tightly bound water monolayer with approximately one water per surface magnesium, and a rather large void between the first

and second peaks of the water density profile. This indicates the water molecules in the first layer are more ordered, and exchange with the water bulk is less frequent. The other is that water molecules in the first layer have two preferred orientations: one with both hydrogens tilted toward the surface, and the other with one hydrogen directed outward and one hydrogen almost parallel to the surface. A less packed second layer exhibits a much broader angular distribution, and the further layers of water are scarcely affected by the surface.

To compare our results with those of McCarthy et al. [23], we integrated the 3D site distribution functions of water along the MgO surface plane. Fig. 1a draws a comparison between the water oxygen density profile following from the 3D-RISM/PLHNC integral equation theory and the simulation. The theory yields a high and rather narrow first peak and then a rather wide void, much as those obtained in the simulation. The hydrogen site distribution function integrated over the unit cell area is plotted in Fig. 1b in comparison with that of water oxygen. Similar to McCarthy et al., we observe splitting of the first peak, with higher probability to find hydrogen atoms pointing towards the surface. The first two peaks of the water oxygen profile yielded by the 3D-RISM theory are situated slightly farther from the surface than those from the simulation. The difference could be attributed to the small number of

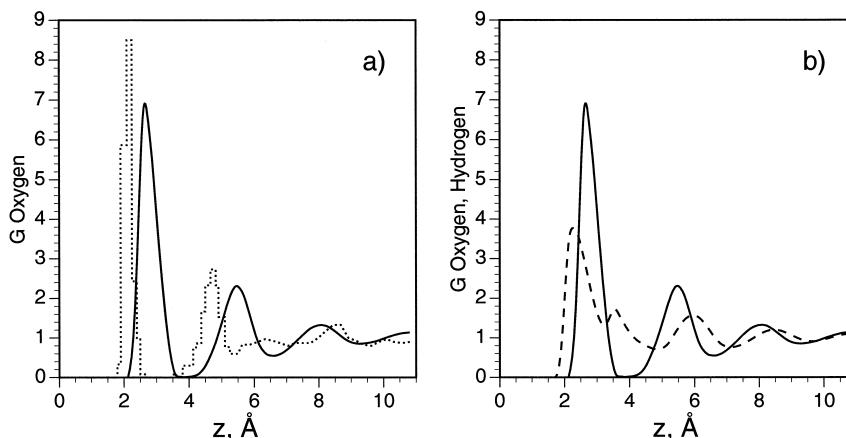


Fig. 1. Transverse average of the water site distributions as a function of the  $z$ -coordinate along the normal to the MgO slab surface. (a) 3D-RISM/PLHNC oxygen site distribution (solid line) vs. the oxygen site profile from the simulation [17] (dotted line). (b) Oxygen and hydrogen site distributions following from the 3D-RISM/PLHNC theory (solid and dashed line, respectively).

water molecules (4 layers) used in modeling the liquid water above the MgO surface and the small time scale in the combined MC/MD simulations [23] (16 ps. for equilibration and 12 ps. for sampling). As mentioned by the authors in Ref. [23], this is also the reason for a rather unphysical third peak in their result. It should be noted that these differences in the first two peaks could also be an artifact related to the well-documented inconsistency in the RISM/HNC theory [35,36]. It manifests in the fact that the correlation between the oxygen and hydrogen site profiles due to the steric constraints is imperfect, especially for the strongly attractive surface–water site poten-

tial under study. Therefore, the maxima of the 3D distribution of water oxygens are somewhat more distant from those of water hydrogens, and hence from the surface, than it follows from the length of the intramolecular OH bond. Despite these differences, the agreement between the two methods on the water density up to 6 Å above the MgO surface is quite good. The number of the water molecules in the first hydration shell, calculated by integration of the oxygen distribution function  $g_O(z)$  over its first peak, was  $N_O = 4.5$  for the 3D-RISM and  $N_O = 4.1$  for the simulation results, which constitutes a difference of < 10%.

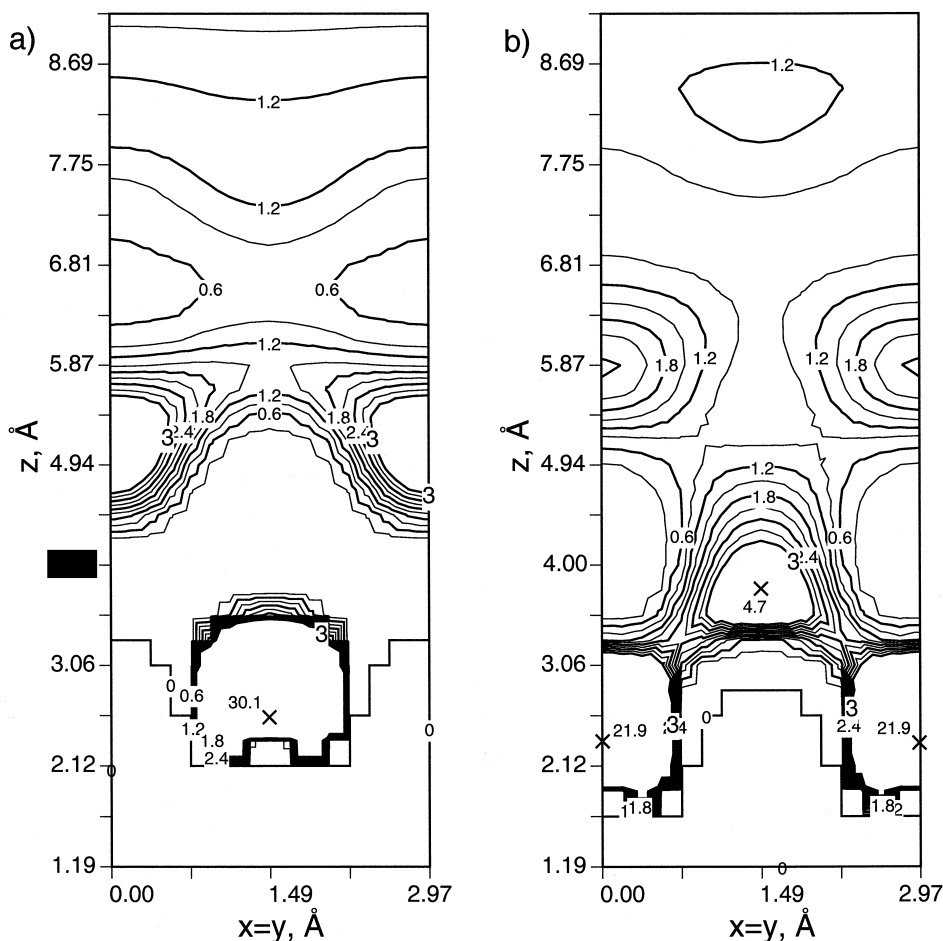


Fig. 2. Three-dimensional distribution functions of oxygen and hydrogen sites (left- and right-hand panel, respectively) in the plane perpendicular to the MgO slab surface and passing through Mg located at  $(x, y, z) = (1.49, 1.49, 0)$  Å, and O situated at  $(0, 0, 0)$  and  $(2.97, 2.97, 0)$  Å. Result of the 3D-RISM/PLHNC theory.

The contour plots of the oxygen and hydrogen site distribution functions in the plane passing through the surface Mg and O atoms in perpendicular to the MgO surface are shown in Fig. 2. These plots show the localization of the oxygen and hydrogen sites similar to that described by McCarthy et al. Oxygen sites of water molecules in the first hydration layer are strongly localized over surface Mg sites (the peak of height  $g_O = 30.1$  at  $z = 2.59$  Å). There are two peaks of hydrogen sites corresponding to such adsorbed water molecules: one is also situated over Mg and shifted outwards from the water oxygen peak by the distance of about the OH bond length, and the other is located closer to the surface at the distance  $z = 2.36$  Å over surface O sites. The former maximum of height  $g_H = 4.7$  corresponds to the localized water molecules with one hydrogen directed away from the surface nearly perpendicular to it and the other slightly tilted toward the surface. The dipole moment of such water molecules is tilted at an angle of  $\sim 60^\circ$ . The hydrogens tilted toward the surface contribute to the latter maximum of the water hydrogen profile over the surface O. However, this latter maximum is formed to a large extent by water molecules tilted with both hydrogens toward the surface and the dipole moment at an angle of  $\sim 18^\circ$

with the normal. Its height,  $g_H = 21.9$ , is substantially bigger than that of the hydrogen peak over the surface Mg,  $g_H = 4.7$ . As a result, the split first peak of the transverse-averaged hydrogen profile in Fig. 1b has the left-hand wing (the closest to the surface) higher than the right-hand one. The above tilts of the dipole moments of water molecules in the first hydration layer perfectly agree with the two peaks of the orientational distributions obtained in the simulation of McCarthy et al.

To demonstrate the in-plane orientations of water molecules, we present also the water oxygen and hydrogen distribution function in the first hydration layer. Fig. 3 shows the water site profiles in the  $xy$ -plane at  $2.5$  Å above the MgO surface, passing through the maximum of the 3D distribution of water oxygens and quite close to the higher maximum of water hydrogens. Evident are the oxygen enrichment region above the Mg atom in the center of the cell, at coordinates  $(x, y) = (1.49, 1.49$  Å), and the strong depletion of water oxygen above the surface oxygen atom in the corners of the cell. Notice that the oxygen maxima are connected with small spikes at the bridge adsorption positions between the surface oxygens. The distribution of water hydrogens is exactly opposite: the high maximum over the surface O

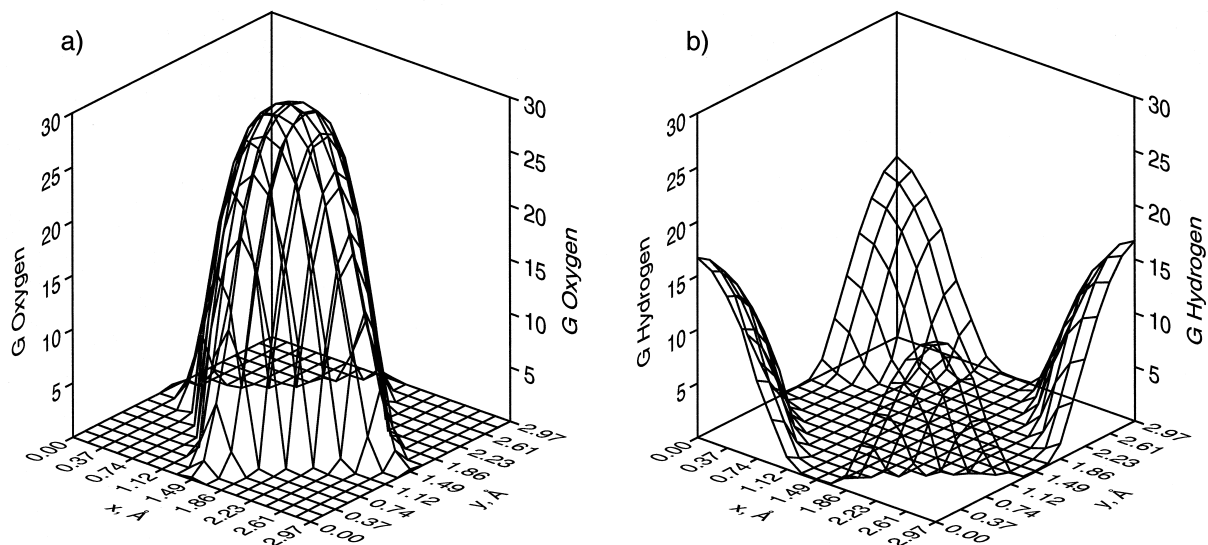


Fig. 3. Three-dimensional distributions of oxygen and hydrogen sites in the plane  $z = 2.5$  Å over the MgO surface (left- and right-hand panel, respectively).

and the strong depletion over Mg. Hence, those hydrogens of water molecules adsorbed in the first hydration layer that are tilted towards the surface are all directed to the surface oxygen atoms.

The ordering in the second hydration layer is essentially weaker, as is evident from Fig. 2. The most striking structural feature is that the maximum of the water oxygen distribution is now located over the surface oxygen. The distance from the surface is about  $z = 5 \text{ \AA}$ , which is just a little more than that of the first hydration layer maximum of water hydrogens over Mg. We can conclude that driven by the highly ordered first hydration layer, water molecules in the second layer tend to follow the close packing of a FCC structure. The second layer maximum of the hydrogen site profile is situated just over the oxygen one at a separation a little smaller than the OH bond length, and is wider and lower. It is due to the water molecules with the dipole moment directed predominantly outward from the surface or somewhat tilted to the normal. Again, this is in agreement with the results of the simulation of McCarthy et al.

## 5. Conclusions

We have presented an examination on the accuracy of the 3D-RISM integral equation theory in modeling liquid structure above a mineral oxide surface. In comparison to the water structure above the MgO(100) surface, obtained in computer simulations by McCarthy et al., we conclude that the 3D-RISM theory provides a cost-effective methodology for modeling liquid structure at a metal oxides–water interface, and can be incorporated in a self-consistent description of chemical processes at the interface. Work is now underway in investigating the origin of the void between the first and second layers of water at the interface as well as improvements on the 3D-RISM approach.

## Acknowledgements

This work is supported in part by the National Science Foundation to T.N.T., and by the Grant-in-Aid for Scientific Research on Priority Area

of “Electrochemistry of Ordered Interface”, No.09237265, from the Japanese Ministry of Education, Science, Sports and Culture to A.K. and F.H.

## References

- [1] J.R. Rustad, A.R. Felmy, B.P. Hay, *Geochim. Cosmochim. Acta* 60 (1996) 1553.
- [2] E.V. Stefanovich, T.N. Truong, *J. Chem. Phys.* 106 (1997) 7700.
- [3] M.A. Johnson, E.V. Stefanovich, T.N. Truong, *J. Phys. Chem.* 102 (1998) 6391.
- [4] J.P. Hansen, I.R. McDonald, *Theory of Simple Liquids*. 2nd edn., Academic Press, London, 1986.
- [5] D. Chandler, H.C. Andersen, *J. Chem. Phys.* 57 (1972) 1930.
- [6] F. Hirata, P.J. Rossky, *Chem. Phys. Lett.* 83 (1981) 329.
- [7] F. Hirata, B.M. Pettitt, P.J. Rossky, *J. Chem. Phys.* 77 (1982) 509.
- [8] F. Hirata, P.J. Rossky, B.M. Pettitt, *J. Chem. Phys.* 78 (1983) 4133.
- [9] F. Hirata, *Bull. Chem. Soc. Jpn.* 71 (1998) 1483.
- [10] D. Chandler, J.D. McCoy, S.J. Singer, *J. Chem. Phys.* 85 (1986) 5971.
- [11] D. Chandler, J.D. McCoy, S.J. Singer, *J. Chem. Phys.* 85 (1986) 5977.
- [12] C.M. Cortis, P.J. Rossky, R.A. Friesner, *J. Chem. Phys.* 107 (1997) 6400.
- [13] D. Beglov, B. Roux, *J. Phys. Chem. B* 101 (1997) 7821.
- [14] A. Kovalenko, F. Hirata, *Chem. Phys. Lett.* 290 (1998) 237.
- [15] A. Kovalenko, S. Ten-no, F. Hirata, *J. Comput. Chem.* 20 (1999) 928.
- [16] A. Kovalenko, F. Hirata, *J. Phys. Chem. B* 103 (1999) 7942.
- [17] A. Kovalenko, F. Hirata, *J. Chem. Phys.* 110 (1999) 10095.
- [18] S. Ten-no, F. Hirata, S. Kato, *Chem. Phys. Lett.* 214 (1993) 391.
- [19] S. Ten-no, F. Hirata, S. Kato, *J. Chem. Phys.* 100 (1994) 7443.
- [20] H. Sato, F. Hirata, S. Kato, *J. Chem. Phys.* 105 (1996) 1546.
- [21] H. Sato, F. Hirata, *J. Am. Chem. Soc.* 121 (1999) 2460.
- [22] S. Maw, H. Sato, S. Ten-no, F. Hirata, *Chem. Phys. Lett.* 276 (1997) 20.
- [23] M.I. McCarthy, G.K. Schenter, C.A. Shamehorn, J.B. Nicholas, *J. Phys. Chem.* 100 (1996) 16989.
- [24] B.M. Pettitt, P.J. Rossky, *J. Chem. Phys.* 77 (1982) 1451.
- [25] M.P. Allen, D.J. Tildesley, *Computer Simulation of Liquids*, Oxford University Press, Oxford, 1987.
- [26] H.J.C. Berendsen, J.P.M. Postma, W.F. von Gunsteren, J. Hermans, in: B. Pullman (Ed.), *Intermolecular Forces*, Reidel, Dordrecht, 1981.
- [27] F. Hirata, J. Levy, *J. Phys. Chem.* 91 (1987) 4788.
- [28] W.H. Press, B.P. Flannery, S.A. Teukolsky, W.T. Vetterling, *Numerical Recipes*. Cambridge University Press, New York, 1986.

- [29] J.D. Talman, *J. Comput. Phys.* 29 (1978) 35.
- [30] P.J. Rossky, H.L. Friedman, *J. Chem. Phys.* 72 (1980) 5694.
- [31] P. Pulay, *Chem. Phys. Lett.* 73 (1980) 393.
- [32] P. Pulay, *J. Comput. Chem.* 3 (1982) 556.
- [33] T.P. Hamilton, P. Pulay, *J. Chem. Phys.* 84 (1986) 5728.
- [34] M. Kawata, C.M. Cortis, R.A. Friesner, *J. Chem. Phys.* 108 (1998) 4426.
- [35] D. Chandler, *Mol. Phys.* 31 (1976) 1213.
- [36] P.T. Cummings, C.G. Gray, D.E. Sullivan, *J. Phys. A: Math. Gen.* 14 (1981) 1483.